

Chapter 7

Positron Collisions with Atoms and Ions

In this chapter we extend our discussion of multichannel R -matrix theory of electron collisions with atoms and atomic ions given in [Chaps. 5](#) and [6](#) to consider positron collisions with these targets. Since the positron is distinguishable from the target electrons, we no longer have to antisymmetrize the total wave function with respect to interchange of the positron coordinates with those of the target electrons. However, this simplification is balanced by the additional channels that have to be included where the incident positron combines with one of the target electrons to form a bound state of the positron–electron system, called positronium (Ps). In this respect, positron collisions with atoms and ions have similarities to electron–molecule collisions which we will consider in [Chap. 11](#) where rearrangement processes corresponding to dissociation and dissociative attachment can occur. A further process that can occur in positron collisions with atoms and ions is where the incident positron annihilates with one of the target electrons with the emission of γ -rays providing a further important test of collision theory. Also processes where positronium atoms are incident on atomic targets are of increasing interest both experimentally and theoretically.

The processes involved in positron and positronium collisions with atoms and ions clearly provide new challenges for both experiment and theory. This has stimulated new developments in the measurement of positron and positronium collision cross sections and in the theory and calculation of positron– and positronium–atom collision cross sections, where applications of R -matrix theory by Walters et al. [[949–953](#)] have been particularly successful. Reviews of these developments and applications have been written by Armour and Humbertson [[23](#)], Laricchia [[576](#)] and Surko et al. [[898](#)]. They have also been discussed in the proceedings of conferences edited by Surko and Gianturco [[897](#)] and by Gribakin and Walters [[423](#)].

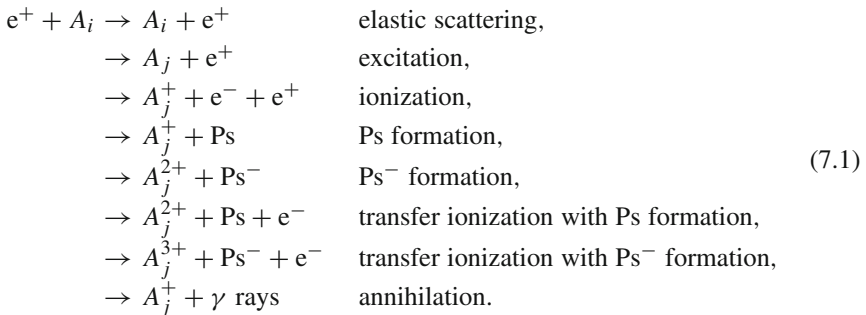
We commence in [Sect. 7.1](#) with a general discussion of the processes that can occur in positron and positronium collisions with atoms and atomic ions. We then consider the new extensions to multichannel R -matrix theory of electron collisions with atoms and ions, considered in [Chaps. 5](#) and [6](#), to enable the channels corresponding to positronium collisions to be included in the theory. Finally, in [Sect. 7.2](#) we present the results of some recent positron and positronium collision calculations using R -matrix theory.

7.1 Multichannel R -Matrix Theory

In this section we introduce R -matrix theory of positron and positronium collisions with atoms and atomic ions by summarizing in Sect. 7.1.1 the various processes that can occur and we compare and contrast these processes with those that occur in electron collisions with atoms and atomic ions discussed in Chap. 5. We also consider the form of the Schrödinger equation which describes positron or positronium collisions with an atom or atomic ion and we discuss the partitioning of configuration space into internal, external and asymptotic regions. We then consider in turn the solution in the internal region in Sect. 7.1.2, in the external region in Sect. 7.1.3 and in the asymptotic region in Sect. 7.1.4 yielding the K -matrix, S -matrix and cross sections for positron and positronium collisions with atoms and ions.

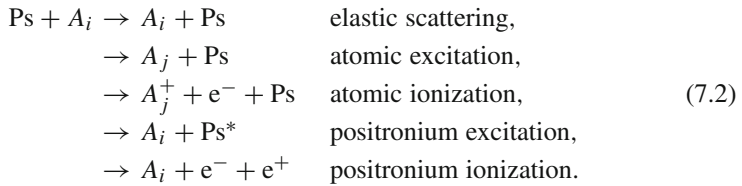
7.1.1 Introduction

In collisions of positrons with atoms and atomic ions the following processes can occur:



The positronium atom (Ps) in (7.1), which can be formed in an excited state, consists of a bound state of the positron and a target electron and is formally the same as the hydrogen atom but with a reduced mass of 0.5 a.u. rather than 1 a.u. Consequently, Ps bound states are classified in the same way as those of atomic hydrogen but with half the energy of the corresponding states, i.e. $E_{n\ell m} = -0.25 n^{-2}$ a.u., where n is the principal quantum number. Positronium can be formed in two spin states, referred to as “ortho” where the positron and electron spins are in the triplet state and as “para” where the two spins are in the singlet state. An interesting discussion of the electron–positron system has been given by Jauch and Rohrlich [499] and recent detailed quantum electrodynamic calculations of Ps lifetimes have been discussed by Kniehl and Penin [539]. In the work of Kniehl and Penin it was shown that the para-positronium 1s state decays predominantly into two photons with a lifetime of 0.125 ns and the ortho-positronium 1s state decays predominantly into three photons with a lifetime of 142 ns. As a result of the relatively long lifetime of ortho-positronium, monoenergetic energy-tunable beams of ortho-positronium

have been developed and the following elastic, inelastic and positronium ionization (fragmentation) collision processes have been studied:



Returning to (7.1), we have also included the process where a positronium negative ion Ps^- is formed which can also occur in positronium collisions. Wheeler [962] showed that Ps could bind an electron to form a negative ion Ps^- , which is the analogue of H^- , and recent values of its binding energy and lifetime are 0.3267 eV and 0.477 ns, respectively [351]. Finally, we observe that the last process listed in (7.1), where the incident positron is annihilated with the emission of γ -rays, is sufficiently weak that it can be ignored in calculating cross sections for the previous positron collision processes listed in (7.1). However, the annihilation rate, which is proportional to the probability of finding the positron and an atomic electron at the same position in space, provides a further important test of the validity of the approximations made in collision theory and calculations.

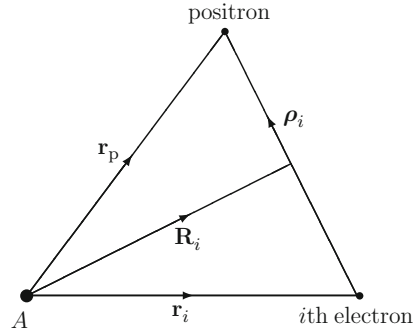
We observe that the essential distinction between electron and positron collisions with atoms and ions is that in the former case the Pauli exclusion principle means that the wave function must be antisymmetrized with respect to the colliding electron and the target electrons, whereas in the latter case the strong attractive interaction between the positron and the target electrons causes the target atom to be strongly distorted at low incident energies. It follows that short-range correlation effects are more important in low-energy positron collisions than in low-energy electron collisions. As a result the additional complexity of using antisymmetrized wave functions in electron collisions is replaced by the greater importance of correlation effects in positron collisions. While these effects can be represented by including additional terms in the expansion of the collision wave function at energies below the positronium formation threshold, they are most appropriately represented by including positronium formation channels in the expansion of the collision wave function, even if results are only required for positron–atom collision channels.

We consider next the form of the Schrödinger equation which describes positron or positronium collisions with an atom or atomic ion with nuclear charge number Z . For light atomic targets, where relativistic effects can be neglected, we must solve the time-independent Schrödinger equation

$$H_{N+p}\Psi = E\Psi, \tag{7.3}$$

where H_{N+p} is the non-relativistic Hamiltonian corresponding to a positron moving in the field of an N -electron atom or a positronium atom moving in the field of an $(N - 1)$ -electron ion. In order to determine explicit expressions for H_{N+p} and Ψ

Fig. 7.1 Jacobi coordinates for positron–atom and positronium–ion collisions, where the i th target atom electron is captured to form positronium



in (7.3) we introduce a Jacobi system of coordinates illustrated in Fig. 7.1, where in this figure \mathbf{r}_p and \mathbf{r}_i are the vector coordinates of the positron and the i th electron in the atom with respect to the atomic nucleus labelled A which is assumed to be infinitely heavy and which is chosen as the origin of coordinates. Also, $\boldsymbol{\rho}_i$ and \mathbf{R}_i in Fig. 7.1 are defined by

$$\boldsymbol{\rho}_i = \mathbf{r}_p - \mathbf{r}_i, \quad \mathbf{R}_i = \frac{1}{2}(\mathbf{r}_p + \mathbf{r}_i). \quad (7.4)$$

We can write H_{N+p} in two distinct forms, the first corresponding to positron–atom collisions and the second corresponding to positronium–ion collisions. In the first form

$$H_{N+p} = H_N - \frac{1}{2}\nabla_p^2 + \frac{Z}{r_p} - \sum_{i=1}^N \frac{1}{\rho_i}, \quad (7.5)$$

where H_N is the non-relativistic atomic Hamiltonian defined by (5.3) with $N + 1$ replaced by N , $-\frac{1}{2}\nabla_p^2$ is the positron kinetic energy operator and the remaining two terms on the right-hand side of (7.5) are the potential interaction of the positron with the atomic nucleus, with charge number Z , and with the N target electrons, respectively.

In the second form corresponding to positronium–ion collisions, one of the N target atom electrons is captured to form positronium. When the i th electron is captured, the Hamiltonian can be written as

$$H_{N+p} = H_{N-i} + H_{pi} - \frac{1}{4}\nabla_{R_i}^2 + V_{N-i pi}. \quad (7.6)$$

In this equation, H_{N-i} is the residual $(N - 1)$ -electron ion Hamiltonian which is defined by

$$H_{N-i} = \sum_{\substack{j=1 \\ j \neq i}}^N \left(-\frac{1}{2} \nabla_j^2 - \frac{Z}{r_j} \right) + \sum_{\substack{j > j'=1 \\ j, j' \neq i}}^N \frac{1}{|\mathbf{r}_j - \mathbf{r}_{j'}|}, \quad (7.7)$$

H_{pi} is the positronium atom Hamiltonian, formed by the positron and the i th captured electron, which is defined by

$$H_{pi} = \nabla_{\rho_i}^2 - \frac{1}{\rho_i}, \quad (7.8)$$

$-\frac{1}{4} \nabla_{R_i}^2$ is the positronium atom kinetic energy operator defined relative to the atomic nucleus and $V_{N-i pi}$ is the potential interaction between the residual $(N-1)$ -electron ion and the positronium atom, which is defined by

$$V_{N-i pi} = -\frac{Z}{r_i} + \frac{Z}{r_p} + \sum_{\substack{j=1 \\ j \neq i}}^N \frac{1}{|\mathbf{r}_j - \mathbf{r}_i|} - \sum_{\substack{j=1 \\ j \neq i}}^N \frac{1}{\rho_j}, \quad (7.9)$$

where in the above equations p refers to the positron and i to the i th electron captured by the positron to form the positronium atom. It follows from the indistinguishability of the N atomic electrons that the Hamiltonian defined by (7.6) is invariant with respect to interchange of any pair of the N electrons.

In order to solve (7.3) using multichannel R -matrix theory we partition configuration space into internal, external and asymptotic regions, as illustrated in Fig. 7.2, which we will see is analogous to the partitioning of configuration space in non-adiabatic electron-molecule collision theory shown in Fig. 11.4. The positron-atom complex in the internal region where all the particles are strongly interacting, defined by $0 \leq r_p \leq a_0$ and $0 \leq R_i \leq A_0$, $i = 1, \dots, N$, can dissociate into both positron-atom collision channels and positronium-ion collision channels. The radius a_0 is chosen so that the amplitudes of the target atom states of interest are negligible for $r_p \geq a_0$ and the radius A_0 is chosen so that the amplitudes of the positronium atom and the target ion states of interest have negligible overlap for $R_i \geq A_0$, $i = 1, \dots, N$. We discuss the solution in the internal region in Sect. 7.1.2. In the external region, corresponding to positron-atom collisions where $a_0 \leq r_p \leq a_p$ and positronium-ion collisions where $A_0 \leq R_N \leq A_q$, the scattered positron and positronium atom move in the long-range multipole potentials of the residual atom or ion, where from symmetry we need to only consider the motion of the positronium atom formed by the positron and the N th target atom electron. In this region the potential interaction between the scattered particles and the residual atom or ion is strong and must be treated by solving the resultant differential equations using accurate numerical propagation methods, as discussed in Sect. 7.1.3. Finally, in the asymptotic region where for positron-atom collisions $r_p \geq a_p$ and for positronium-ion collisions $R_N \geq A_q$, the solutions can be obtained using asymptotic expansions in each of these regions which enable the K -matrix and S -matrix

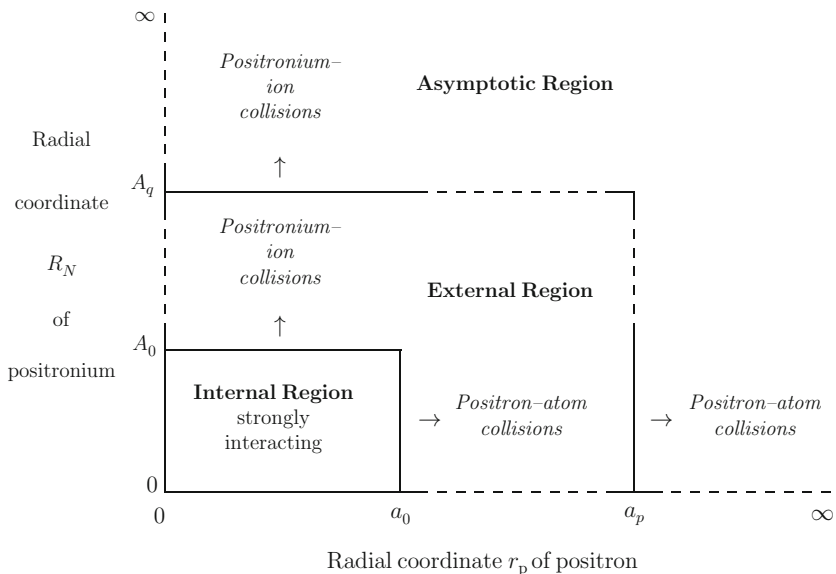


Fig. 7.2 Partitioning of configuration space in R -matrix theory of positron–atom and positronium–ion collisions, where the N th target atom electron is captured to form positronium

to be determined, as discussed in Sect. 7.1.4. We now consider the solution in the internal, external and asymptotic regions in turn.

7.1.2 Internal Region Solution

We consider first the solution of the non-relativistic Schrödinger equation (7.3) in the internal region in Fig. 7.2 for each set of conserved quantum numbers Λ defined below. In analogy with expansions (5.5) and (5.6) adopted in electron–atom collisions we expand the positron–atom collision wave function as follows:

$$\Psi_{jE}^{\Lambda}(\mathbf{X}_N; \mathbf{x}_p) = \sum_k \psi_k^{\Lambda}(\mathbf{X}_N; \mathbf{x}_p) A_{kj}^{\Lambda}(E). \quad (7.10)$$

In this equation

$$\mathbf{X}_N \equiv \mathbf{x}_1, \mathbf{x}_2, \dots, \mathbf{x}_N, \quad (7.11)$$

where $\mathbf{x}_i \equiv \mathbf{r}_i \sigma_i$ represents the space and spin coordinates of the i th electron, $\mathbf{x}_p \equiv \mathbf{r}_p \sigma_p$ represents the space and spin coordinates of the positron, j labels the linearly independent solutions of (7.3), ψ_k^{Λ} are energy-independent basis functions and $A_{kj}^{\Lambda}(E)$ are energy-dependent expansion coefficients which depend on the asymptotic boundary conditions satisfied by the wave function Ψ_{jE}^{Λ} at the energy E . Also

in (7.10), Λ represents the conserved quantum numbers in the collision defined by

$$\Lambda \equiv \alpha L S M_L M_S m_p \pi, \quad (7.12)$$

where L and M_L are the total orbital angular momentum quantum numbers of the positron–atom and positronium–ion collision processes, S and M_S are the total electron spin angular momentum quantum numbers of the target atom and m_p is the spin magnetic quantum number of the positron, which are separately conserved, π is the total parity and α represents any further quantum numbers which are conserved in the collision. Unlike the conserved quantum numbers Γ in electron–atom collisions, defined by (2.58), we have not coupled the spin of the positron to that of the target atom since the positron is distinguishable from the target electrons and hence, in the absence of relativistic spin–orbit interactions, M_S and m_p are separately conserved in the positron–atom collision. It follows that the collision wave function Ψ_{jE}^Λ and the basis functions ψ_k^Λ in (7.10) are antisymmetric with respect to interchange of any pair of the space and spin coordinates $\mathbf{x}_i \equiv \mathbf{r}_i \sigma_i$, $i = 1, \dots, N$, of the target electrons, but are not antisymmetrized with respect to interchange of the space and spin coordinates $\mathbf{x}_p \equiv \mathbf{r}_p \sigma_p$ of the positron with those of the target electrons.

We now expand the basis functions ψ_k^Λ in (7.10) in the form

$$\begin{aligned} \psi_k^\Lambda(\mathbf{X}_N; \mathbf{x}_p) &= \sum_{i=1}^n \sum_{j=1}^{n_c} \bar{\Phi}_i^\Lambda(\mathbf{X}_N; \hat{\mathbf{r}}_p \sigma_p) r^{-1} u_{ij}^0(r_p) a_{ijk}^\Lambda \\ &+ \mathcal{A}_N \sum_{i=1}^m \sum_{j=1}^{m_c} \bar{\Theta}_i^\Lambda(\mathbf{X}_{N-1}; \boldsymbol{\rho}_N \sigma_N \sigma_p; \hat{\mathbf{R}}_N) \\ &\times R_N^{-1} v_{ij}^0(R_N) b_{ijk}^\Lambda \\ &+ \sum_{i=1}^b \chi_i^\Lambda(\mathbf{X}_N; \mathbf{x}_p) c_{ik}^\Lambda, \quad k = 1, \dots, n_t, \end{aligned} \quad (7.13)$$

where $n_t = nn_c + mm_c + b$ is the number of linearly independent basis functions included in these expansions. The first expansion on the right-hand side of (7.13) corresponds to positron–atom collisions, the second expansion corresponds to positronium–ion collisions, where the N th electron is captured to form positronium leaving the remaining $N - 1$ electrons in the residual ion and the third expansion is over quadratically integrable functions which are included for completeness and to represent correlation effects. Also in (7.13), $\bar{\Phi}_i^\Lambda$ and u_{ij}^0 are the channel functions and radial continuum basis orbitals corresponding to positron–atom collisions and $\bar{\Theta}_i^\Lambda$ and v_{ij}^0 are the channel functions and radial continuum basis orbitals corresponding to positronium–ion collisions, which are discussed below. Finally, in (7.13) \mathcal{A}_N is the antisymmetrization operator which ensures that each term in the second expansion is antisymmetric with respect to interchange of the space and spin

coordinates of any pair of the N electrons taking part in the collision. In analogy with (2.46) \mathcal{A}_N is defined by

$$\mathcal{A}_N = N^{-1/2} \left(1 - \sum_{i=1}^{N-1} P_{iN} \right), \quad (7.14)$$

where P_{iN} is the operator which interchanges the space and spin coordinates of electrons labelled i and N .

We observe that the expansions over the channel functions $\bar{\Phi}_i^\Lambda$ and $\bar{\Theta}_i^\Lambda$ in (7.13) may both include pseudostates representing the continuum in positron–atom collisions and positronium–ion collisions, respectively. We have seen in Chaps. 2, 5 and 6 that the inclusion of pseudostates is required both to accurately represent the polarizability of the target by the incident particle at low energies and to allow for ionization at intermediate energies. As a result, in principle, the two expansions span the same configuration space, which could lead to instability in the solution if close to complete sets of target basis functions are included in each expansion. However, in practical calculations both expansions are truncated to a finite number of basis functions and hence any difficulty due to over completeness usually does not arise. Retaining both expansions together with the expansion over quadratically integrable functions χ_i^Λ in (7.13) then gives faster convergence and enables positron collision and positronium formation cross sections to be defined and accurately calculated at low and intermediate energies.

The channel functions $\bar{\Phi}_i^\Lambda$ in (7.13) corresponding to positron–atom collisions are constructed by coupling the orbital angular momentum of the antisymmetrized N -electron target atom wave functions Φ_i^N with the orbital angular momentum of the scattered positron as follows:

$$\bar{\Phi}_i^\Lambda(\mathbf{X}_N; \hat{\mathbf{r}}_p \sigma_p) = \sum_{M_i m_i} (L_i M_i \ell_i m_i | L M_L) \Phi_i^N(\mathbf{X}_N) Y_{\ell_i m_i}(\theta_p, \phi_p) \chi_{\frac{1}{2} m_p}(\sigma_p),$$

$$i = 1, \dots, n, \quad (7.15)$$

where the boundary radius a_0 of the internal region in Fig. 7.2 is chosen so that the target atom wave functions $\Phi_i^N(\mathbf{X}_N)$ are negligible for $r_i \geq a_0$, $i = 1, \dots, N$.

The channel functions $\bar{\Theta}_i^\Lambda$ in (7.13) corresponding to positronium–ion collisions are constructed by coupling the orbital and spin angular momenta of the antisymmetrized residual atomic ion wave function $\Phi_i^{N-1}(\mathbf{X}_{N-1})$ with the orbital and spin angular momenta of the positronium atom wave function, where we assume that the N th atomic electron and the positron form the positronium atom. We now introduce the following wave function describing the positron and the N th atomic electron:

$$\xi_i(\boldsymbol{\rho}_N; \sigma_N \sigma_p) = \phi_i(\boldsymbol{\rho}_N) \chi_{\frac{1}{2} m_N}(\sigma_N) \chi_{\frac{1}{2} m_p}(\sigma_p), \quad (7.16)$$

where $\phi_i(\boldsymbol{\rho}_N)$ is the space part of the positronium atom wave function, $\chi_{\frac{1}{2}m_N}(\sigma_N)$ is the N th atomic electron spin function and $\chi_{\frac{1}{2}m_p}(\sigma_p)$ is the positron spin function. Using (A.20), we can rewrite (7.16) as a linear combination of singlet and triplet positronium atom spin functions $\chi_{s_i m_s}(\sigma_N \sigma_p)$ as follows:

$$\xi_i(\boldsymbol{\rho}_N; \sigma_N \sigma_p) = \sum_{s_i} \left(\frac{1}{2} m_N \frac{1}{2} m_p |s_i m_s \right) \phi_i(\boldsymbol{\rho}_N) \chi_{s_i m_s}(\sigma_N \sigma_p), \quad (7.17)$$

where the Clebsch–Gordan coefficients in this equation are defined in Sect. A.1. The channel functions $\bar{\Theta}_i^A$ in (7.13) are then defined by

$$\begin{aligned} & \bar{\Theta}_i^A(\mathbf{X}_{N-1}; \boldsymbol{\rho}_N \sigma_N \sigma_p; \hat{\mathbf{R}}_N) \\ &= \sum_{M'_L m'_\ell} \sum_{M_K m_j} \sum_{M'_S m_s} (L'_i M'_L \ell'_i m'_\ell | K_i M_K) (K_i M_K j_i m_j | L M_L) \\ & \quad \times (S'_i M'_S s_i m_s | S M_S) \Phi_i^{N-1}(\mathbf{X}_{N-1}) \phi_i(\boldsymbol{\rho}_N) \\ & \quad \times \chi_{s_i m_s}(\sigma_N \sigma_p) Y_{j_i m_j}(\theta_N, \phi_N), \quad i = 1, \dots, m, \end{aligned} \quad (7.18)$$

where the boundary radius A_0 of the internal region in Fig. 7.2 is chosen so that the overlap of the residual atomic ion wave functions $\Phi_i^{N-1}(\mathbf{X}_{N-1})$ and the positronium wave function $\phi_i(\boldsymbol{\rho}_N)$ is negligible for $R_N \geq A_0$.

The angular momentum coupling scheme that we have adopted in (7.18), in defining the channel functions $\bar{\Theta}_i^A$ in (7.13), is summarized in Fig. 7.3. The orbital and spin angular momentum quantum numbers of the residual atomic ion are L'_i , M'_L , S'_i , M'_S , the orbital angular momentum quantum numbers of the positronium atom are ℓ'_i , m'_ℓ and the spin magnetic quantum numbers of the captured N th electron and the positron are m_N and m_p , respectively. Then K_i and M_K are intermediate angular momentum quantum numbers obtained by coupling the orbital angular momenta of the residual ion denoted by L'_i and M'_L with the orbital angular

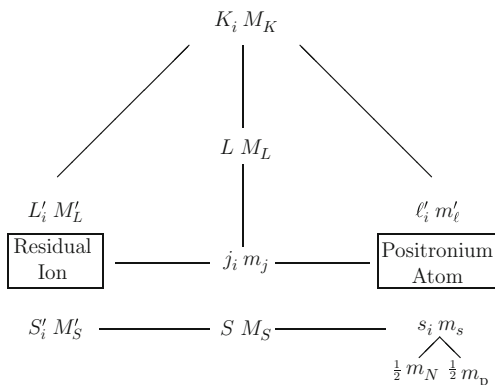


Fig. 7.3 Positronium–ion orbital and spin angular momentum coupling scheme defining the positronium wave function ξ_i in (7.17) and the channel functions $\bar{\Theta}_i^A$ in (7.18)

momenta of the positronium atom denoted by ℓ'_i and m'_ℓ , j_i and m_j are the orbital angular momentum quantum numbers describing the orbital motion of the positronium atom relative to the residual ion and L and M_L are the total conserved orbital angular momentum quantum numbers of the positronium atom and the residual ion. Also S and M_S are the total conserved electron spin angular momentum quantum numbers of the positronium atom and the residual ion obtained by coupling the electron spin angular momentum of the residual ion denoted by S'_i and M'_S with the spin angular momentum of the positronium atom denoted by s_i and m_s . We also remember from (7.16) and (7.17) that electron and positron spins are coupled to yield the positronium atom spin quantum numbers s_i and m_s . Finally, we observe that the total parity π in (7.12), defined by

$$\pi = \pi_i(-1)^{\ell_i} = \pi'_i(-1)^{\ell'_i+j_i}, \quad (7.19)$$

is conserved in the collision where π_i is the parity of the N -electron target atom and π'_i is the parity of the residual atomic ion.

The zero-order radial continuum basis orbitals $u_{ij}^0(r_p)$ and $v_{ij}^0(R_N)$ in (7.13) are defined over the ranges $0 \leq r_p \leq a_0$ and $0 \leq R_N \leq A_0$, respectively, in the internal region defined in Fig. 7.2. In practice the continuum basis orbitals can be calculated using a homogeneous boundary condition method similar to that described in Sect. 5.3.1 for electron–atom collisions (e.g. [531]). However, since the positron is distinguishable from the electrons in the target atom or residual ion, the Lagrange orthogonalization procedure adopted for electron–atom collisions is not required. Hence, the continuum basis orbitals in (7.13) can be obtained by solving equations analogous to (5.75) with the right-hand side set zero. In the case of $u_{ij}^0(r_p)$, corresponding to the positron–atom collision channels, the potential $U_0(r)$ in (5.75) can be taken to be the repulsive static potential of the target atom ground state. In the case of $v_{ij}^0(R_N)$, corresponding to the positronium–ion collision channels, the potential $U_0(r)$ in (5.75) can be taken to be zero. This is justified for positron collisions with alkali metal atoms since the diagonal elements of the potential corresponding to positronium collisions with the resultant closed-shell ion are zero.

The final step in the definition of the quantities in (7.13) is to determine the coefficients a_{ijk}^Λ , b_{ijk}^Λ and c_{ik}^Λ . This is achieved by diagonalizing the operator $H_{N+p} + \mathcal{L}_r + \mathcal{L}_R$ in the basis ψ_k^Λ defined by (7.13) where the integral is taken over the internal region in Fig. 7.2 as follows:

$$\langle \psi_k^\Lambda | H_{N+p} + \mathcal{L}_r + \mathcal{L}_R | \psi_{k'}^\Lambda \rangle_{\text{int}} = E_k^\Lambda \delta_{kk'}, \quad k, k' = 1, \dots, n_t. \quad (7.20)$$

In this equation we have introduced the Bloch operator for positron–atom collision channels in (7.13) defined by

$$\mathcal{L}_r = \frac{1}{2} \delta(r_p - a_0) \left(\frac{d}{dr_p} - \frac{b_0 - 1}{r_p} \right), \quad (7.21)$$

which corresponds to the form of the Hamiltonian defined by (7.5), and the Bloch operator for positronium–ion collision channels in (7.13) defined by

$$\mathcal{L}_R = \frac{1}{4} \sum_{i=1}^N \delta(R_i - A_0) \left(\frac{d}{dR_i} - \frac{B_0 - 1}{R_i} \right), \quad (7.22)$$

which corresponds to the form of the Hamiltonian defined by (7.6), where b_0 in (7.21) and B_0 in (7.22) are arbitrary constants. It follows that $H_{N+p} + \mathcal{L}_r + \mathcal{L}_R$ is hermitian in the basis of quadratically integrable functions (7.13), satisfying arbitrary boundary conditions on the surface of the internal region in Fig. 7.2 where $r_p = a_0$ and $R_i = A_0$, $i = 1, \dots, N$.

The solution of (7.3) in the internal region for each set of conserved quantum numbers Λ defined by (7.12) can be obtained by rewriting (7.3) as follows:

$$(H_{N+p} + \mathcal{L}_r + \mathcal{L}_R - E)\Psi^\Lambda = (\mathcal{L}_r + \mathcal{L}_R)\Psi^\Lambda, \quad (7.23)$$

which has the formal solution

$$\Psi^\Lambda = (H_{N+p} + \mathcal{L}_r + \mathcal{L}_R - E)^{-1}(\mathcal{L}_r + \mathcal{L}_R)\Psi^\Lambda. \quad (7.24)$$

The spectral representation of the Green's function in this equation can be written in terms of the basis functions ψ_k^Λ defined by (7.13) and (7.20). We obtain

$$|\Psi^\Lambda\rangle = \sum_{k=1}^{n_t} |\psi_k^\Lambda\rangle \frac{1}{E_k^\Lambda - E} \langle \psi_k^\Lambda | \mathcal{L}_r + \mathcal{L}_R | \Psi^\Lambda \rangle. \quad (7.25)$$

We then project (7.25) onto the n channel functions $\overline{\Phi}_i^\Lambda$, $i = 1, \dots, n$, defined by (7.15) and evaluate it on the boundary $r_p = a_0$ and project (7.25) onto the m channel functions $\overline{\Theta}_i^\Lambda$, $i = 1, \dots, m$, defined by (7.18) and evaluate it on the boundary $R_N = A_0$. We obtain, after using (7.21) and (7.22)

$$\begin{aligned} F_i^\Lambda(a_0) &= \sum_{j=1}^n R_{ij}^\Lambda(E) \left(a_0 \frac{dF_j^\Lambda}{dr_p} - b_0 F_j^\Lambda \right)_{r_p=a_0} \\ &\quad + \sum_{j=1}^m R_{i,j+n}^\Lambda(E) \left(A_0 \frac{dG_j^\Lambda}{dR_N} - B_0 G_j^\Lambda \right)_{R_N=A_0}, \quad i = 1, \dots, n \end{aligned} \quad (7.26)$$

and

$$G_i^A(A_0) = \sum_{j=1}^n R_{i+n}^A j(E) \left(a_0 \frac{dF_j^A}{dr_p} - b_0 F_j^A \right)_{r_p=a_0} + \sum_{j=1}^m R_{i+n}^A j+n(E) \left(A_0 \frac{dG_j^A}{dR_N} - B_0 G_j^A \right)_{R_N=A_0}, \quad i = 1, \dots, m. \quad (7.27)$$

In (7.26) and (7.27), the reduced radial functions $F_i^A(r_p)$, which correspond to positron–atom collisions, are obtained by projecting the total wave function Ψ^A onto the channel functions $\bar{\Phi}_i^A$ defined by (7.15) as follows:

$$F_i^A(r_p) = \langle r_p^{-1} \bar{\Phi}_i^A | \Psi^A \rangle', \quad i = 1, \dots, n, \quad (7.28)$$

and the reduced radial functions $G_i^A(R_N)$, which correspond to positronium–ion collisions, are obtained by projecting the total wave function Ψ^A onto the channel functions $\bar{\Theta}_i^A$ defined by (7.18) as follows:

$$G_i^A(R_N) = \langle R_N^{-1} \bar{\Theta}_i^A | \Psi^A \rangle', \quad i = 1, \dots, m. \quad (7.29)$$

The R -matrices in (7.26) and (7.27) are then combined into a generalized R -matrix defined by

$$R_{ij}^A(E) = \frac{1}{2a_0} \sum_{k=1}^{n_t} \frac{w_{ik}^A w_{jk}^A}{E_k^A - E}, \quad i = 1, \dots, n+m, \quad j = 1, \dots, n \quad (7.30)$$

and

$$R_{ij}^A(E) = \frac{1}{4A_0} \sum_{k=1}^{n_t} \frac{w_{ik}^A w_{jk}^A}{E_k^A - E}, \quad i = 1, \dots, n+m, \quad j = n+1, \dots, n+m, \quad (7.31)$$

where the surface amplitudes in these equations are defined by

$$w_{ik}^A = \langle r_p^{-1} \bar{\Phi}_i^A | \psi_k^A \rangle'_{r_p=a_0} = \sum_{j=1}^{n_t} u_{ij}^0(a_0) a_{ijk}^A, \quad i = 1, \dots, n, \quad k = 1, \dots, n_t \quad (7.32)$$

and

$$\begin{aligned} w_{i+n k}^{\Lambda} &= \langle R_N^{-1} \bar{\Theta}_i^{\Lambda} | \psi_k^{\Lambda} \rangle'_{R_N=A_0} \\ &= \sum_{j=1}^{m_c} v_{ij}^0(A_0) b_{ijk}^{\Lambda}, \quad i = 1, \dots, m, \quad k = 1, \dots, n_t, \end{aligned} \quad (7.33)$$

which follow from (7.13). The primes on the Dirac brackets in the above equations mean that the integrations are carried out over all coordinates except the radial coordinate r_p in (7.28) and (7.32) and except the radial coordinate R_N in (7.29) and (7.33).

Equations (7.26) and (7.27) are the basic equations which result from the solution of the Schrödinger equation (7.3) describing positron–atom collisions and positronium–ion collisions in the internal region. The R -matrix defined by (7.30) and (7.31) is determined at all energies by diagonalizing $H_{N+p} + \mathcal{L}_r + \mathcal{L}_R$ in the basis defined by (7.13) to yield the eigenenergies E_k^{Λ} in (7.20) for each set of conserved quantum numbers Λ . If the zero-order radial continuum basis orbitals $u_{ij}^0(r_p)$ and $v_{ij}^0(R_N)$ in (7.13) are calculated using the homogeneous boundary condition method then a Buttle correction to the diagonal elements of the R -matrix must be applied as described in Sect. 5.3.2. Having determined the R -matrix, (7.26) and (7.27) then provide the boundary conditions satisfied by the solution of the equations describing positron–atom collisions and positronium–ion collisions in the external region described in the next section.

7.1.3 External Region Solution

The external region, defined in Fig. 7.2, is divided into two sub-regions corresponding to positron–atom collision channels and positronium–ion collision channels. We assume that the corresponding radii a_0 and A_0 are chosen large enough so that for the channels of interest the corresponding wave functions in these two external sub-regions have negligible overlap and can therefore be treated independently.

In the external sub-region corresponding to positron–atom collisions, we expand the total wave function in terms of channel functions $\bar{\Phi}_i^{\Lambda}$ defined by (7.15) as follows:

$$\Psi_{jE}^{\Lambda}(\mathbf{X}_N; \mathbf{r}_p \sigma_p) = \sum_{i=1}^n \bar{\Phi}_i^{\Lambda}(\mathbf{X}_N; \hat{\mathbf{r}}_p \sigma_p) r_p^{-1} F_{ij}^{\Lambda}(r_p), \quad (7.34)$$

where j labels the linearly independent solutions. We then substitute this expansion into the Schrödinger equation (7.3), where the Hamiltonian H_{N+p} is defined by (7.5), and project this equation onto the channel functions $\bar{\Phi}_i^{\Lambda}$. We then find that

the reduced radial functions $F_{ij}^A(r_p)$ in (7.34) satisfy the following set of coupled second-order differential equations:

$$\left(\frac{d^2}{dr_p^2} - \frac{\ell_i(\ell_i + 1)}{r_p^2} - \frac{2(Z - N)}{r_p} + k_i^2 \right) F_{ij}^A(r_p) = 2 \sum_{i'=1}^n V_{ii'}^A(r_p) F_{i'j}^A(r_p),$$

$$i = 1, \dots, n, \quad r_p \geq a_0, \quad (7.35)$$

where ℓ_i is the orbital angular momentum of the scattered positron, Z is the nuclear charge number, N is the number of target electrons and k_i^2 is the square of the wave number of the scattered positron defined by

$$k_i^2 = 2(E - \bar{e}_i^A), \quad i = 1, \dots, n, \quad (7.36)$$

where

$$\bar{e}_i^A = \langle r_p^{-1} \bar{\Phi}_i^A(\mathbf{X}_N; \hat{\mathbf{r}}_p \sigma_p) | H_N | r_p^{-1} \bar{\Phi}_i^A(\mathbf{X}_N; \hat{\mathbf{r}}_p \sigma_p) \rangle, \quad i = 1, \dots, n. \quad (7.37)$$

Finally in (7.35), $V_{ii'}^A(r_p)$ is the potential matrix defined in analogy with (2.66) by

$$V_{ii'}^A(r_p) = \langle r_p^{-1} \bar{\Phi}_i^A(\mathbf{X}_N; \hat{\mathbf{r}}_p \sigma_p) \left| - \sum_{k=1}^N \frac{1}{\rho_k} + \frac{N}{r_p} \right| r_p^{-1} \bar{\Phi}_{i'}^A(\mathbf{X}_N; \hat{\mathbf{r}}_p \sigma_p) \rangle',$$

$$i, i' = 1, \dots, n. \quad (7.38)$$

We see that (7.35) has the same general form as the coupled second-order differential equations (5.29) describing electron–atom collisions in the external region. This is because the electron exchange terms in electron–atom collisions are confined to the internal region and hence the potential in (5.29) only describes the long-range interaction between the electron and the atom. The differences between (7.35) and (5.29) then arise because the positron has positive charge and the electron negative charge. This results in the change in sign in the long-range Coulomb potential $-2(Z - N)/r_p$ and in the sign of the potential matrix $V_{ii'}^A(r_p)$. It follows that

$$V_{ii'}^A(r_p) = -V_{ii'}^\Gamma(r), \quad r_p = r, \quad i, i' = 1, \dots, n, \quad (7.39)$$

where in the external region the conserved quantum numbers in positron–atom collisions represented by A are the same as the conserved quantum numbers in electron–atom collisions represented by Γ . Hence we find that the potential matrix $V_{ii'}^A(r_p)$ in (7.35) can be written as a summation over inverse powers of r_p where the coefficients in the expansion have the opposite sign to those given in (5.30).

In the external sub-region in Fig. 7.2 corresponding to positronium–ion collisions, we expand the total wave function in terms of channel functions $\bar{\Theta}_i^A$ defined by (7.18) as follows:

$$\Psi_{jE}^A(\mathbf{X}_{N-1}; \boldsymbol{\rho}_N \sigma_N \sigma_p; \mathbf{R}_N) = \sum_{i=1}^m \bar{\Theta}_i^A(\mathbf{X}_{N-1}; \boldsymbol{\rho}_N \sigma_N \sigma_p; \hat{\mathbf{R}}_N) R_N^{-1} G_{ij}^A(R_N), \quad (7.40)$$

where j , which has the same meaning as in (7.34), labels the linearly independent solutions. We then substitute this expansion into the Schrödinger equation (7.3), where the Hamiltonian H_{N+p} is now defined by (7.6) and where, as in Fig. 7.2, we assume that the N th target atom electron has been captured to form positronium. After projecting (7.3) onto the channel functions $\bar{\Theta}_i^A$ we then find that the reduced radial functions $G_{ij}^A(\mathbf{R}_N)$ in (7.40) satisfy the following coupled second-order differential equations:

$$\left(\frac{d^2}{dR_N^2} - \frac{j_i(j_i + 1)}{R_N^2} + K_i^2 \right) G_{ij}^A(R_N) = 4 \sum_{i'=1}^m U_{ii'}^A(R_N) G_{i'j}^A(R_N), \quad i = 1, \dots, m, \quad R_N \geq A_0. \quad (7.41)$$

In this equation j_i , defined in Fig. 7.3, is the angular momentum quantum number in the i th channel corresponding to the orbital motion of the positronium atom relative to the residual ion. Also in (7.41) K_i^2 is the square of the wave number K_i of the positronium atom in the i th channel defined by

$$K_i^2 = 4 [E - (E_{N-1})_i - (E_{pN})_i], \quad (7.42)$$

where $(E_{N-1})_i$ is the energy of the residual $(N-1)$ -electron ion in the i th channel defined by

$$(E_{N-1})_i = \langle \Phi_i^{N-1}(\mathbf{X}_{N-1}) | H_{N-1} | \Phi_i^{N-1}(\mathbf{X}_{N-1}) \rangle, \quad i = 1, \dots, m, \quad (7.43)$$

and $(E_{pN})_i$ is the energy of the positronium atom in the i th channel defined by

$$(E_{pN})_i = \langle \phi_i(\boldsymbol{\rho}_N) \chi_{s_i m_s}(\sigma_N \sigma_p) | H_{pN} | \phi_i(\boldsymbol{\rho}_N) \chi_{s_i m_s}(\sigma_N \sigma_p) \rangle, \quad i = 1, \dots, m, \quad (7.44)$$

where H_{N-1} and H_{pN} are defined by (7.7) and (7.8), respectively, with i replaced by N . Finally in (7.41), $U_{ii'}^A(R_N)$ is the potential matrix defined by

$$U_{ii'}^A(R_N) = \langle R_N^{-1} \bar{\Theta}_i^A(\mathbf{X}_{N-1}; \boldsymbol{\rho}_N \sigma_N \sigma_p; \hat{\mathbf{R}}_N) | V_{N-1 pN} | R_N^{-1} \bar{\Theta}_{i'}^A(\mathbf{X}_{N-1}; \boldsymbol{\rho}_N \sigma_N \sigma_p; \hat{\mathbf{R}}_N) \rangle, \quad i, i' = 1, \dots, m, \quad (7.45)$$

where $V_{N-1 pN}$ is the potential interaction between the residual ion and the positronium atom defined by (7.9), with i replaced by N .

Having determined the coupled second-order differential equations (7.35) and (7.41), satisfied by the functions $F_{ij}^A(r_p)$ and $G_{ij}^A(R_N)$, respectively, the generalized $(n+m) \times (n+m)$ -dimensional R -matrix \mathbf{R}^A defined by (7.30) and (7.31) can then be propagated outwards from the boundaries $r_p = a_0$ and $R_N = A_0$ to the outer boundaries $r_p = a_p$ and $R_N = A_q$ in Fig. 7.2 using the procedure described in Appendix E.6. The R -matrix at the outer boundaries then provides the boundary condition for the solution in the asymptotic region, discussed in Sect. 7.1.4.

7.1.4 Asymptotic Region Solution

The solution of (7.3) in the asymptotic region, where $r_p \geq a_p$ and $R_N \geq A_q$ in Fig. 7.2, proceeds using an extension of the method adopted in the asymptotic region in electron–atom collisions, discussed in Sect. 5.1.4. First, we assume that we have chosen the radii a_p and A_q in Fig. 7.2 large enough that the asymptotic expansion methods discussed in Appendix F.1 can be used to obtain accurate linearly independent solutions of (7.35) when $r_p \geq a_p$ and of (7.41) when $R_N \geq A_q$. Following our discussion in Sect. 5.1.4, we then assume that the n positron–atom collision channels corresponding to (7.35), which we distinguish by a bar, are ordered so that

$$\bar{k}_1^2 \geq \bar{k}_2^2 \geq \dots \geq \bar{k}_n^2, \quad (7.46)$$

where at the energy E of interest the first n_a channels are open with $\bar{k}_i^2 \geq 0$ and the last n_b channels are closed with $\bar{k}_i^2 < 0$, where $n_a + n_b = n$. We then determine $n + n_a$ linearly independent asymptotic solutions of (7.35), which are regular as $r_p \rightarrow \infty$ and which satisfy the following asymptotic boundary conditions:

$$\begin{aligned} \bar{s}_{ij}(r_p) &\underset{r_p \rightarrow \infty}{\sim} \bar{k}_i^{-1/2} \sin \bar{\theta}_i \delta_{ij}, & i = 1, \dots, n, & \quad j = 1, \dots, n_a, \\ \bar{c}_{ij}(r_p) &\underset{r_p \rightarrow \infty}{\sim} \bar{k}_i^{-1/2} \cos \bar{\theta}_i \delta_{ij}, & i = 1, \dots, n, & \quad j = 1, \dots, n_a, \\ \bar{c}_{ij}(r_p) &\underset{r_p \rightarrow \infty}{\sim} \exp(-\bar{\phi}_i) \delta_{ij}, & i = 1, \dots, n, & \quad j = n_a + 1, \dots, n, \end{aligned} \quad (7.47)$$

where $\bar{\theta}_i$ and $\bar{\phi}_i$ are defined by equations analogous to (5.38), (5.39), (5.40) and (5.41). Also, we assume that the m positronium–ion collision channels corresponding to (7.41), which we distinguish by a tilde, are ordered so that

$$\tilde{k}_1^2 \geq \tilde{k}_2^2 \geq \dots \geq \tilde{k}_m^2, \quad (7.48)$$

where at the energy E of interest the first m_a channels are open with $\tilde{k}_i^2 \geq 0$ and the last m_b channels are closed with $\tilde{k}_i^2 < 0$, where $m_a + m_b = m$. We then determine

$m + m_a$ linearly independent asymptotic solutions of (7.41), which are regular as $R_N \rightarrow \infty$ and which satisfy the following asymptotic boundary conditions:

$$\begin{aligned}\tilde{s}_{ij}(R_N) &\underset{R_N \rightarrow \infty}{\sim} \tilde{k}_i^{-1/2} \sin \tilde{\theta}_i \delta_{ij}, & i = 1, \dots, m, & \quad j = 1, \dots, m_a, \\ \tilde{c}_{ij}(R_N) &\underset{R_N \rightarrow \infty}{\sim} \tilde{k}_i^{-1/2} \cos \tilde{\theta}_i \delta_{ij}, & i = 1, \dots, m, & \quad j = 1, \dots, m_a, \\ \tilde{c}_{ij}(R_N) &\underset{R_N \rightarrow \infty}{\sim} \exp(-\tilde{\phi}_i) \delta_{ij}, & i = 1, \dots, m, & \quad j = m_a + 1, \dots, m, \end{aligned} \quad (7.49)$$

where $\tilde{\theta}_i$ and $\tilde{\phi}_i$ are also defined by equations analogous to (5.38), (5.39), (5.40) and (5.41).

We observe that at an energy E where n_a channels of (7.35) and m_a channels of (7.41) are open, we can determine $n_a + m_a$ linearly independent physical solutions of the combined internal and external region equations which vanish at the origin and which are finite at infinity. In analogy with (5.42), these solutions can be written in terms of the $n + n_a$ asymptotic solutions defined by (7.47) and the $m + m_a$ asymptotic solutions defined by (7.49) as follows

$$\mathcal{F}^A(\rho) = \mathbf{s}(\rho) + \mathbf{c}(\rho)\mathbf{N}^A, \quad r_p \geq a_p, \quad R_N \geq A_q, \quad (7.50)$$

where we have written $\mathbf{s}(\rho)$ to represent $\bar{\mathbf{s}}(r)$ or $\tilde{\mathbf{s}}(R_N)$ and $\mathbf{c}(\rho)$ to represent $\bar{\mathbf{c}}(r)$ or $\tilde{\mathbf{c}}(R_N)$ and where the variable ρ represents r_p in the channels corresponding to (7.35) and R_N in the channels corresponding to (7.41). It follows that in (7.50)

$$\begin{aligned}\mathcal{F}^A(\rho) &\text{ has dimension } (n + m) \times (n_a + m_a), \\ \mathbf{s}(\rho) &\text{ has dimension } (n + m) \times (n_a + m_a), \\ \mathbf{c}(\rho) &\text{ has dimension } (n + m) \times (n + m), \\ \mathbf{N}^A &\text{ has dimension } (n + m) \times (n_a + m_a). \end{aligned} \quad (7.51)$$

Also, so that the ordering of open and closed channels in (7.50) is the same as in (5.42), we have re-ordered the channels in (7.50) so that the first $n_a + m_a$ channels are open and the last $n_b + m_b$ channels are closed. Hence the ordering of open and closed channels in (7.50) is as follows:

$$\begin{aligned}\text{channels } 1 \text{ to } n_a &\equiv n_a \text{ open channels in (7.35),} \\ \text{channels } n_a + 1 \text{ to } n_a + m_a &\equiv m_a \text{ open channels in (7.41),} \\ \text{channels } n_a + m_a + 1 \text{ to } n + m_a &\equiv n_b \text{ closed channels in (7.35),} \\ \text{channels } n + m_a + 1 \text{ to } n + m &\equiv m_b \text{ closed channels in (7.41).} \end{aligned} \quad (7.52)$$

In analogy with (5.43), the matrix \mathbf{N}^A in (7.50) can then be rewritten in the form

$$\mathbf{N}^A = \begin{bmatrix} \mathbf{K}^A \\ \mathbf{L}^A \end{bmatrix}, \quad (7.53)$$

where \mathbf{K}^Λ is the $(n_a + m_a) \times (n_a + m_a)$ -dimensional K -matrix which couples the $n_a + m_a$ open channels in (7.35) and (7.41) and \mathbf{L}^Λ is a subsidiary $(n_b + m_b) \times (n_a + m_a)$ -dimensional matrix which couples the solutions in (7.47) and (7.49) which vanish asymptotically. We see that \mathbf{K}^Λ postmultiplies the first $n_a + m_a$ columns in the matrix $\mathbf{c}(\rho)$ in (7.50) and \mathbf{L}^Λ postmultiplies the last $n_b + m_b$ columns of $\mathbf{c}(\rho)$.

Following our discussion in Sect. 5.1.4, we now express the $(n_a + m_a) \times (n_a + m_a)$ -dimensional K -matrix coupling the open channels in (7.35) and (7.41) in terms of the $(n + m) \times (n + m)$ -dimensional R -matrix \mathbf{R}^Λ , defined on the outer boundaries of the external region $r_p = a_p$ and $R_N = A_q$ in Fig. 7.2, obtained using the propagator method described in Appendix E.6, or an equivalent procedure. The R -matrix on the boundary $r_p = a_p$ and $R_N = A_q$ is then defined in analogy with (E.116) and (E.117) as follows:

$$\begin{aligned} \mathbf{F}^\Lambda(a_p, A_q) &= \mathbf{R}_{11}^\Lambda(a_p, A_q) a_p \mathbf{F}^{\Lambda'}(a_p, A_q) + \mathbf{R}_{12}^\Lambda(a_p, A_q) A_q \mathbf{G}^{\Lambda'}(a_p, A_q), \\ \mathbf{G}^\Lambda(a_p, A_q) &= \mathbf{R}_{21}^\Lambda(a_p, A_q) a_p \mathbf{F}^{\Lambda'}(a_p, A_q) + \mathbf{R}_{22}^\Lambda(a_p, A_q) A_q \mathbf{G}^{\Lambda'}(a_p, A_q), \end{aligned} \quad (7.54)$$

where $\mathbf{F}^{\Lambda'}$ and $\mathbf{G}^{\Lambda'}$ are the derivatives $d\mathbf{F}^\Lambda/dr_p$ and $d\mathbf{G}^\Lambda/dR_N$, respectively.

We now observe that the components of the asymptotic solution \mathcal{F}^Λ , defined by (7.50), and their derivatives, defined by

$$\mathcal{F}^{\Lambda'}(\rho) = \mathbf{s}'(\rho) + \mathbf{c}'(\rho)\mathbf{N}^\Lambda, \quad r_p \geq a_p, \quad R_N \geq A_q, \quad (7.55)$$

correspond on the boundary $r_p = a_p$ and $R_N = A_q$ to solutions (7.54), after appropriate re-ordering corresponding to (7.52). Hence, following our analysis in Sect. 5.1.4, we can substitute the appropriate re-ordered asymptotic solutions \mathcal{F}^Λ and $\mathcal{F}^{\Lambda'}$ defined by (7.50) and (7.55) on the boundary $r_p = a_p$ and $R_N = A_q$ of the external region for the functions \mathbf{F}^Λ and \mathbf{G}^Λ and the derivatives $\mathbf{F}^{\Lambda'}$ and $\mathbf{G}^{\Lambda'}$ in (7.54). This yields a set of $n + m$ linear simultaneous equations with $n_a + n_b$ right-hand sides, which are analogous to (5.46). The solution of these equations then yields the elements of the $(n + m) \times (n_a + m_a)$ -dimensional matrix \mathbf{N}^Λ and hence from (7.53) the $(n_a + m_a) \times (n_a + m_a)$ -dimensional K -matrix \mathbf{K}^Λ .

It follows from (7.50) that the required physical solution matrix $\mathcal{F}^\Lambda(\rho)$ satisfies the asymptotic boundary condition

$$\mathcal{F}^\Lambda(\rho) \underset{\substack{r_p \rightarrow \infty \\ R_N \rightarrow \infty}}{\sim} \mathbf{s}(\rho) + \mathbf{c}(\rho)\mathbf{K}^\Lambda, \quad (7.56)$$

where we remember from (7.52) that the first n_a channels in (7.56) correspond to open positron–atom channels, and the next m_a channels in (7.56) correspond to open positronium–ion channels. Hence the K -matrix \mathbf{K}^Λ couples the n_a open

positron–atom channels and the m_a open positronium–ion channels. The $(n_a + m_a) \times (n_a + m_a)$ -dimensional S -matrix \mathbf{S}^A is then defined in terms of the K -matrix \mathbf{K}^A in the usual way by the matrix equation

$$\mathbf{S}^A = \frac{\mathbf{I} + i\mathbf{K}^A}{\mathbf{I} - i\mathbf{K}^A}. \quad (7.57)$$

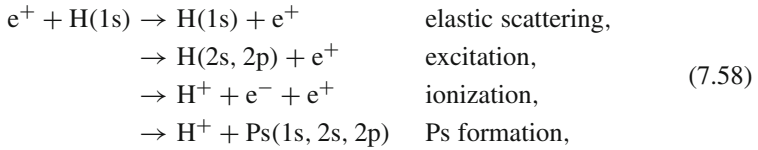
The corresponding T -matrix and cross sections describing transitions between the open positron–atom channels and the open positronium–ion channels can then be determined using the procedure described in Sect. 2.5. The solutions in the internal, external and asymptotic regions in Fig. 7.2 can be determined in a similar way for all relevant conserved quantum numbers A defined by (7.12) enabling the corresponding cross sections for transitions between the open positron–atom and positronium–ion channels to be determined.

7.2 Positron and Positronium Collision Calculations

In recent years detailed positron– and positronium–atom collision calculations have been carried out using R -matrix computer programs, where a major motivation for these theoretical and computational advances has been new developments in experiments. In addition to R -matrix calculations for positron collisions with atomic hydrogen carried out by Higgins et al. [467, 468, 470] and Kernoghan et al. [531, 532] detailed R -matrix calculations have been carried out for positron collisions with “one-electron” alkali metal atoms Li, Na, K, Rb and Cs by McAlinden et al. [607–611], Campbell et al. [202] and Walters et al. [950, 951] and with “two-electron” atoms He, Mg, Ca and Zn by Campbell et al. [202]. Also in recent years there has been a rapid increase in the experimental capability to produce monoenergetic, energy-tunable beams of the longer life ortho-positronium which are used in collision experiments, for example, by Laricchia et al. [574, 575, 577–580], Charlton et al. [215, 216], Zafar et al. [988–990], Garner et al. [362–364], Gilbert et al. [372], Armitage et al. [20] and Brawley et al. [124]. These developments have stimulated considerable interest in the calculation of positronium collisions with atoms and detailed R -matrix calculations have been carried out for positronium collisions with H by Campbell et al. [201] and Blackwood et al. [112–114] and with He, Na, Ar, Kr and Xe by Blackwood et al. [111, 113]. We will discuss examples of these collision calculations in the following sections.

7.2.1 Positron Collisions with H

As our first example we consider R -matrix calculations of positron collisions with atomic hydrogen at low and intermediate energies carried out by Kernoghan et al. [531, 532]. In this work they considered the following processes:



where they compared their results with experimental measurements by Jones et al. [508] and Zhou et al. [1010].

The R -matrix calculations were carried out in the energy range 0–110 eV using a 33-state approximation which included in expansion (7.13) the 1s, 2s and 2p eigenstates of both positronium and atomic hydrogen with 27 atomic hydrogen pseudostates, which represented the hydrogen atom ionization continuum. The results presented in Fig. 7.4 show excellent agreement between the calculations and experiment for the total positronium formation cross section, the ionization cross section and the total cross section over the full range of energies considered, showing that the 33-state calculation can accurately describe the main features of the cross section for positron collisions with the ground state of atomic hydrogen. In particular, the inclusion of pseudostates in this calculation gives an accurate representation of the ionization continuum at intermediate energies.

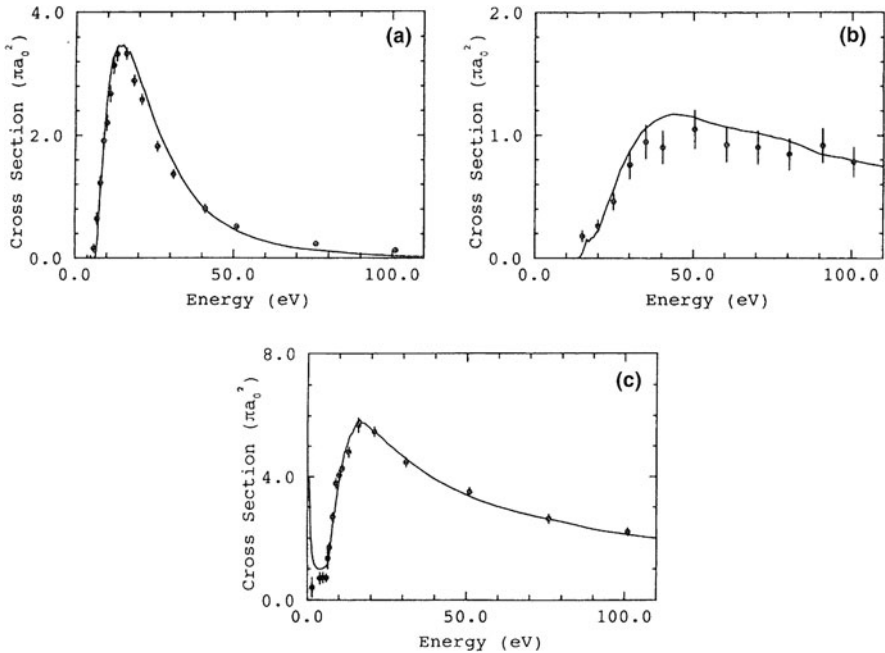


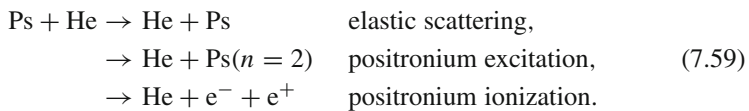
Fig. 7.4 Positron collisions with atomic hydrogen: (a) total positronium formation cross section, (b) ionization cross section, (c) total cross section. *Solid curve*: 33-state calculation [532]; *points*: experimental data from [508, 1010] (Fig. 1 from [953])

7.2.2 Positronium Collisions with He

We consider next R -matrix calculations of positronium collisions with helium atoms where initially the target helium atom is restricted to its $^1S^e$ ground state. This “frozen-target” approximation has been successfully applied by Blackwood et al. [111] to describe elastic scattering, positronium excitation and positronium ionization in the energy range 0–40 eV. However, this work also highlighted significant discrepancies between theory and experiment for low-energy positronium–helium atom collisions. Hence in Sect. 7.2.3 we consider calculations for positronium collisions with helium and hydrogen atoms by Walters et al. [952] which, by including virtual transitions in the target, show the importance of target polarization in low-energy collisions.

7.2.2.1 Frozen-Target Approximation

We consider first R -matrix calculations for positronium collisions with helium atoms carried out by Blackwood et al. [111] who studied the following collision processes:



In this work results from three levels of approximation were reported, where in each case the frozen-target approximation is adopted where only the $^1S^e$ ground state of He was retained in the second expansion in (7.13). In the first static exchange approximation, only the Ps(1s) state and the He($^1S^e$) state were retained in (7.13). In the second nine-state approximation (9ST), the 1s, 2s and 2p eigenstates of Ps together with $\overline{3s}$, $\overline{3p}$, $\overline{3d}$, $\overline{4s}$, $\overline{4p}$, $\overline{4d}$ pseudostates were retained in (7.13). Finally, in the third 22-state approximation (22ST), the 1s, 2s and 2p eigenstates of Ps as well as $\overline{3s-7s}$, $\overline{3p-7p}$, $\overline{3d-7d}$ and $\overline{4f-7f}$ pseudostates were retained in (7.13). In all of these calculations we note that since the target helium atom is restricted to the $^1S^e$ ground state, an ortho-positronium projectile cannot be converted into a para-positronium projectile or vice versa. Hence in this approximation the collision cross sections for ortho-positronium and para-positronium collisions are the same.

We show in Fig. 7.5 the total cross section for the 22ST approximation and its principal components, i.e. the elastic cross section, the positronium ionization (fragmentation) cross section and the positronium excitation cross section to the 2s and 2p states, calculated by Blackwood et al. [111]. The ionization cross section was extracted from the calculation [532, 611] by taking

$$\sigma_{\text{ion}}(\text{Ps}) = \sum_j f_j \sigma_j(\text{Ps}), \tag{7.60}$$

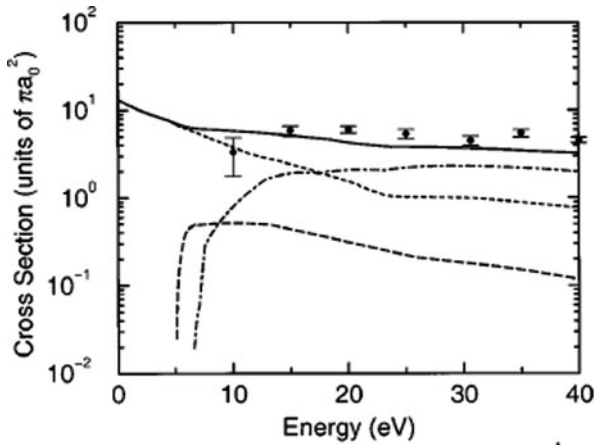


Fig. 7.5 Cross sections for positronium collisions with helium atoms calculated in the 22ST R -matrix approximation by Blackwood et al. [111]. *Solid curve*: total cross section; *short dashed curve*: elastic scattering cross section; *dash-dot curve*: Ps ionization (fragmentation) cross section; *long-dashed curve*: Ps($n=2$) excitation cross section; *solid circles*: total cross section measurements by Garner et al. [362, 363] (Fig. 2 from [111])

where $\sigma_j(\text{Ps})$ is the cross section for exciting the j th positronium pseudostate and f_j is the fraction of this state overlapping the positronium continuum. We see from this figure that the calculated total cross section is in good agreement with the measurements of Garner et al. [362, 363].

We also compare the calculated positronium ionization cross section with later measurements by Armitage et al. [20] and with Born approximation calculations by Biswas and Adhikari [109] in Fig. 7.6. We see from this figure that including pseudostates in the R -matrix calculation gives a good representation of the ionization

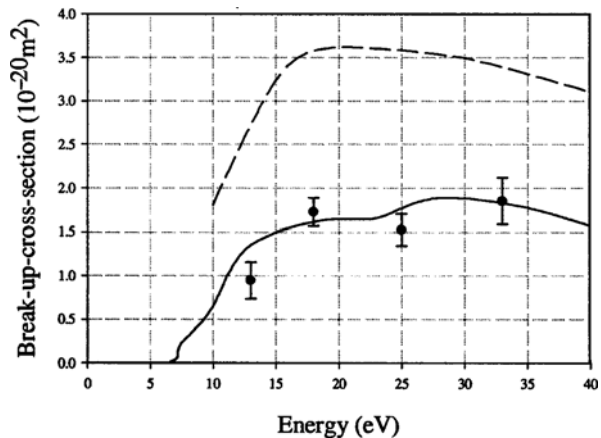


Fig. 7.6 Positronium ionization cross section for positronium collisions with helium atoms. *Solid curve*: R -matrix calculation by Blackwood et al. [111]; *dashed curve*: Born approximation calculation by Biswas and Adhikari [109]; *solid circles*: experimental measurements by Armitage et al. [20] (Fig. 2. from [20])

cross section in this energy range. However, it is also clear from this figure that the Born approximation is, as expected, not accurate at these relatively low energies.

7.2.3 Target Polarization in Positronium Collisions

In order to study the effect of target polarization on low-energy collision cross sections, Walters et al. [952] carried out a series of calculations for positronium collisions with helium and atomic hydrogen targets including excited states and pseudostates in both the expansions of the positronium and target states.

In the case of S-wave positronium collisions with helium, 1s, 2s and 2p eigenstates and $\overline{3s}$, $\overline{3p}$, $\overline{3d}$, $\overline{4s}$, $\overline{4p}$, $\overline{4d}$ pseudostates of Ps together with $1\ ^1S^e$, $2\ ^1S^e$, $2\ ^1P^o$ eigenstates and $3\ ^1S^e$, $3\ ^1P^o$, $3\ ^1D^e$, $4\ ^1S^e$, $4\ ^1P^o$, $4\ ^1D^e$ pseudostates of helium were retained in expansion (7.13) giving a 9Ps9He calculation. In the case of P-wave positronium collisions with helium some numerical instabilities were encountered

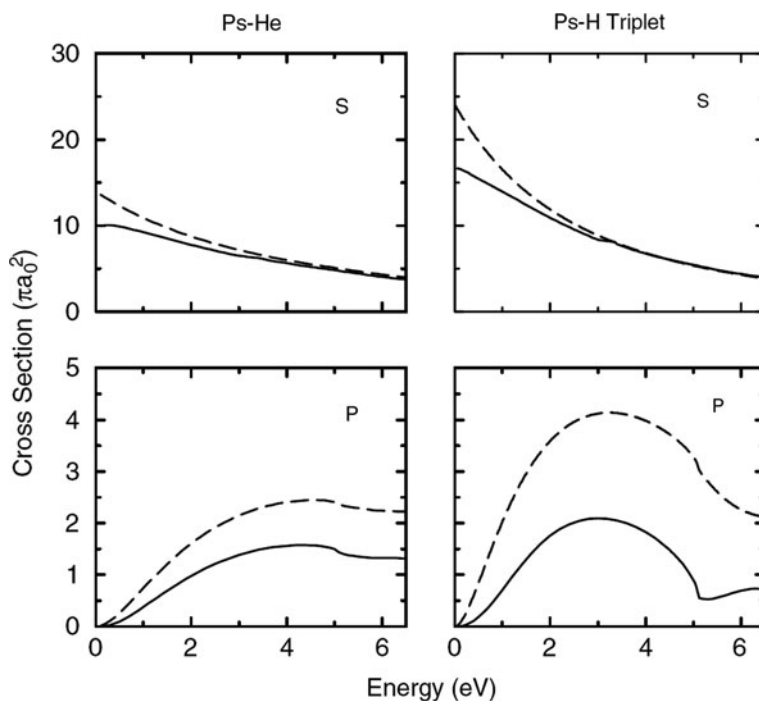


Fig. 7.7 S-wave and P-wave cross sections for Ps(1s) elastic scattering by He($1\ ^1S^e$) and H(1s). The Ps–H cross sections are for collisions in the electron spin triplet state. For He: *solid curve*, 9Ps9He approximation for S-wave and 7Ps7He approximation for P-wave; *dashed curve*, 9Ps1He approximation for S-wave and 7Ps1He approximation for P-wave. For H: *solid curves*, 9Ps9H approximation; *dashed curves*, 9Ps1H approximation for S-wave and for P-wave (Fig. 5 from [952])

so a reduced $7Ps7He$ calculation was adopted in which the positronium and helium D-wave pseudostates were omitted. We compare in Fig. 7.7 the corresponding S- and P-wave Ps–He elastic scattering cross sections with results obtained using frozen He target approximations corresponding to $9Ps1He$ for S-wave and $7Ps1He$ for P-wave scattering. Also shown in Fig. 7.7 are corresponding results for positronium collisions with atomic hydrogen in the triplet electronic spin state. We see from this figure that the results for both atomic hydrogen and helium targets are similar with a significant reduction in the cross section occurring at low energies when virtual transitions in the target are included in the calculation. Also we observe that the reduction is more significant for atomic hydrogen, probably because of the higher excitation energies for the He target.

In conclusion, these calculations show that target polarization plays an important role in low-energy positronium–atom collisions and that virtual transitions of the target must be included to obtain accurate low-energy collision cross sections.